

Supplemental Figure Legends

Fig. S1. Confirming Smad2/3 knockdown.

HUVECs transfected with Smad2 and Smad3 siRNA and Smad2/3 expression assessed by western blotting at the indicated times.

Fig. S2. Confirmation of Nrp1 and Alk5.

(A) ECs after Nrp1 depletion were stimulated with the indicated concentration of TGF β 2 in the absence or presence of FSS at 12 dynes/cm² for 30 min and Smad2/3 activation assayed by western blotting. Values are means \pm SEM, n=3. (B) ECs after Alk5 or Nrp-1 depletion and re-expression were subject to 5 dynes/cm² FSS for 4h, then fixed, stained for Smad2/3 and nuclear translocation assayed as before. Scale bar: 50 μ m. n=80 cells for each group from three independent experiments. *** $P < 0.001$, calculated by one-way ANOVA with Tukey's multiple comparison tests.

Fig S3. Ligands required for flow-induced Smad2/3 activation.

(A) ECs in serum-free medium received the indicated dose of TGF β 2 and were left without flow (static) or exposed to FSS at 12 dynes/cm² for 30min. Smad2/3 phosphorylation was assayed by western blotting and quantified as before. Values are means \pm SEM, N=3. (B) ECs in serum free medium with or without BMP9 at 100 pg/ml were left under static conditions or exposed to FSS at 5 dynes/cm² for 4h. Cells were then fixed, stained for Smad2/3 and

nuclear translocation quantified. Scale bar: 50 μ m. n=80 cells for each group from three independent experiments. **(C)** ECs in serum free medium with or without BMP10 were subject to FSS and Smad2/3 phosphorylation analyzed as in A. N=3. Values are means \pm SEM. * $P < 0.05$, *** $P < 0.001$, ns: not significant, calculated by one-way ANOVA with Tukey's multiple comparison tests.

Fig. S4. Flow velocity after surgery.

Mice were subject to partial ligation of the left carotid artery as described in Methods. Doppler measurement of flow velocity in the operated right (RT) and sham control left (LT) common carotid arteries (CCA) at day 3 after surgery.

Fig. S5. Carotid ligation in the rat.

Rats were subjected to carotid ligation as described in Methods. At 2 weeks after surgery, animals were sacrificed and the common carotid upstream of the ligation fixed, sectioned, and stained as indicated. Upper panels: representative images. Lower panels: quantification of endothelial cell pSmad2 in the nucleus, n=5, calculated by unpaired Student's *t*-test.

Fig. S6. Confirming MEKK3 and KLF2 knockdowns.

Western blots for ECs transfected with control siRNA or siRNA targeting **A.** MEKK3 or **B.** KLF2.

Fig. S7. MEKK3 Knockdown in MAECs

(A) MAECs were transfected with control or MEKK3 siRNA and KD validated by Western blotting. (B) Cells were subjected to FSS at the indicated magnitudes for 12h and immunostained for Smad2/3. Scale bar: 50 μm . (C) Quantification of Smad2/3 nucleus/cytoplasm intensity ratio. $n=100-150$ cells for each group from three independent experiments. $***P < 0.001$, ns: not significant, calculated by one-way ANOVA with Tukey's multiple comparison tests.

Fig. S8. eNOS knockdown.

(A) HUVECs were transfected with control or eNOS siRNA and KD validated by Western blotting. (B) Cells were subjected to FSS at the indicated magnitudes for 12h and immunostained for Smad2/3, Scale bar: 50 μm . (C) Quantification of Smad2/3 nucleus/cytoplasm intensity ratio. $n=100-150$ cells for each group from three independent experiments. $***P < 0.001$, ns: not significant, calculated by one-way ANOVA with Tukey's multiple comparison tests.

Fig. S9. Cyclin-dependent kinase signaling.

(A) Representative images of Smad2/3 staining under static and 25 dynes/cm² FSS in HUVECs treated with DMSO, CDK inhibitor AT7519 (500

nM) or Flavopiridol HCl (200 nM). Scale bar: 50 μ m. **(B)** Quantification of Smad2/3 nucleus/cytoplasm intensity ratio. n=100 cells for each group from three independent experiments. *** $P < 0.001$, ns: not significant, calculated by one-way ANOVA with Tukey's multiple comparison tests. Cells treated with **(C)** Flavopiridol (200 nM), **(D)** AT7519 (500 nM) or **(E)** AZD4573 (50 nM) as above then were analyzed for Smad2/3 linker phosphorylation by Western blotting.

Fig S10. Cdk2 activation time course.

ECs expressing the Cdk2 reporter plus mCherry-H2B were subject to flow at 5 dynes/cm² and 25 dynes/cm² for the indicated times. Cytoplasmic localization of the reporter indicates delayed activation that is minimal at 45 min. Scar bar: 50 μ m. Arrowheads: cells with cytoplasmic reporter.

Fig. S11. FSS signaling network.

Diagram summarizing the FSS magnitude-dependent signaling network that regulates inward vessel remodeling. FSS activates two independent pathways that together result in a Smad2/3 signaling that is maximal at low FSS. Flow activates Smad2/3 with high sensitivity through Alk5 and Nrp1 to phosphorylate Smad2/3 C-termini. Activation of the MEKK3/Klf2 pathway occurs at higher FSS and inhibits Smad2/3 nuclear translocation mainly through induction of Klf2 and activation of CDK2, without affecting C-terminal

phosphorylation. MEKK3 activation also induces Smad2/3 linker phosphorylation at short times after onset of flow independent of Klf2 (not in the figure) but Klf2 is the major pathway once flow is established. Smad2/3 signaling then induces artery inward remodeling.

Figure S1. Knockdown confirmation

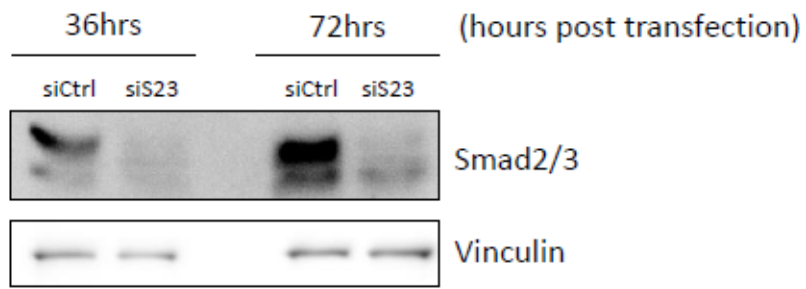


Figure S2. Confirmation of Nrp1 and Alk5

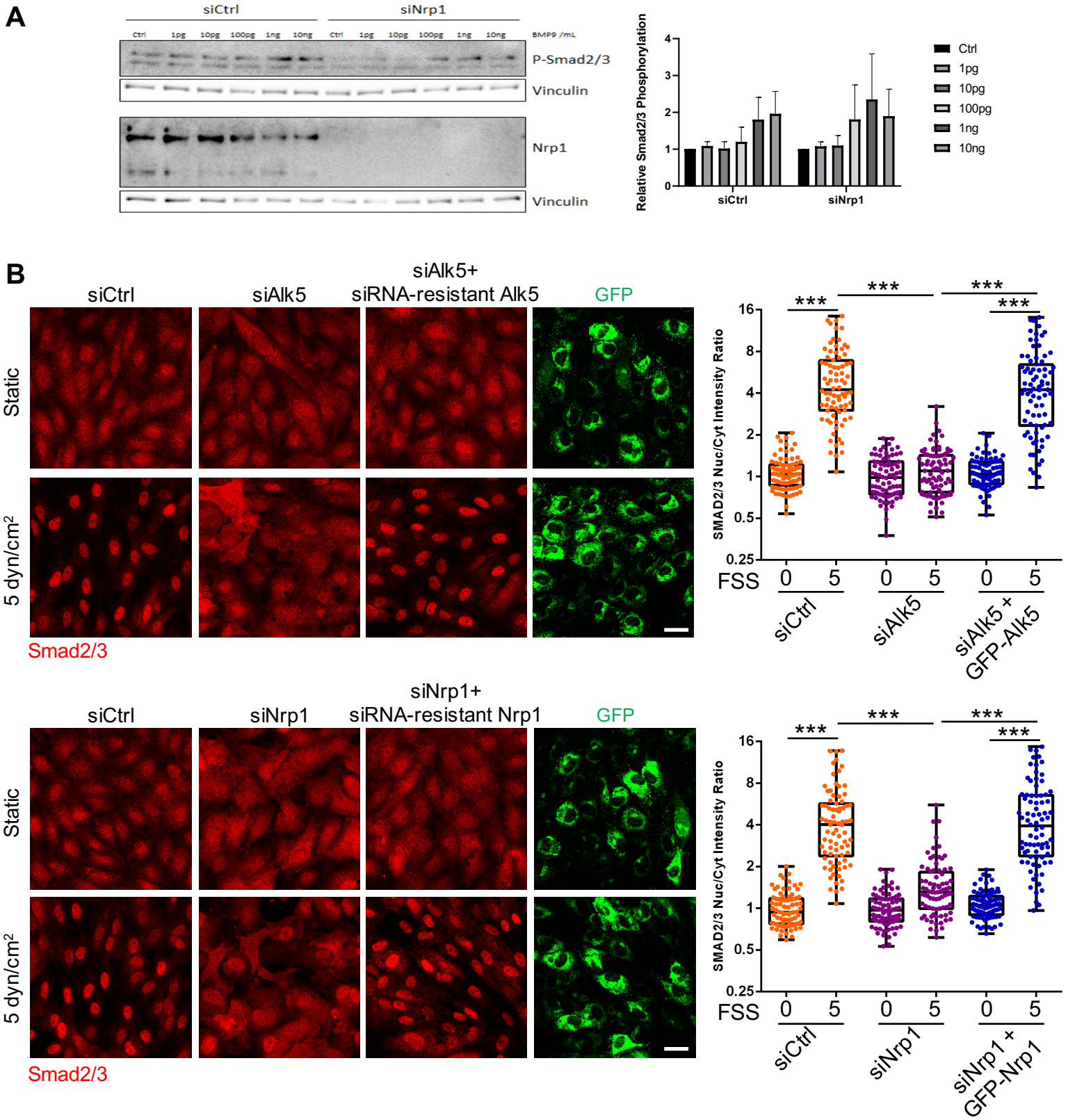


Figure S3. Ligands for flow-induced Smad2/3 activation

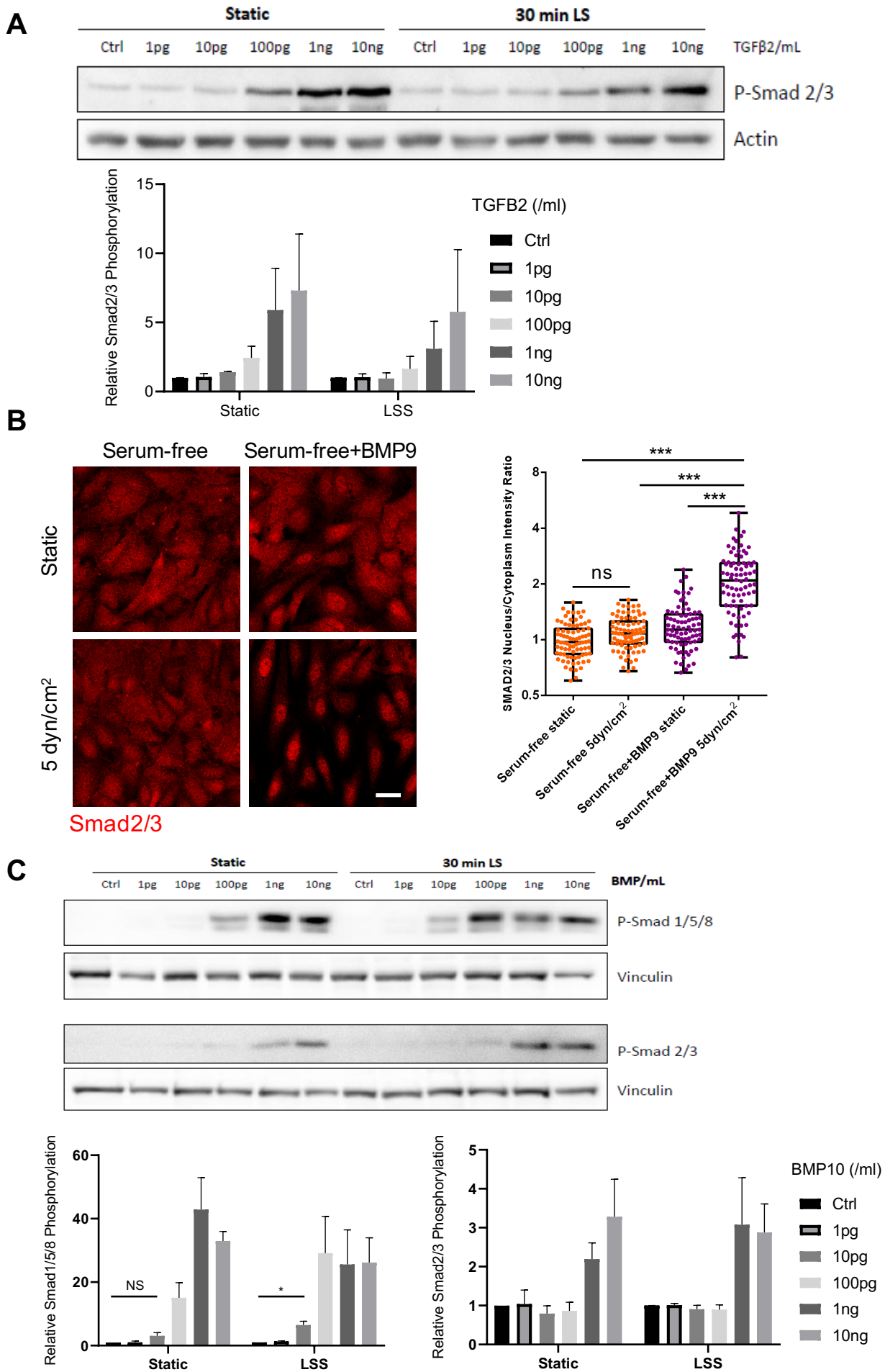


Figure S4. Flow velocity after surgery

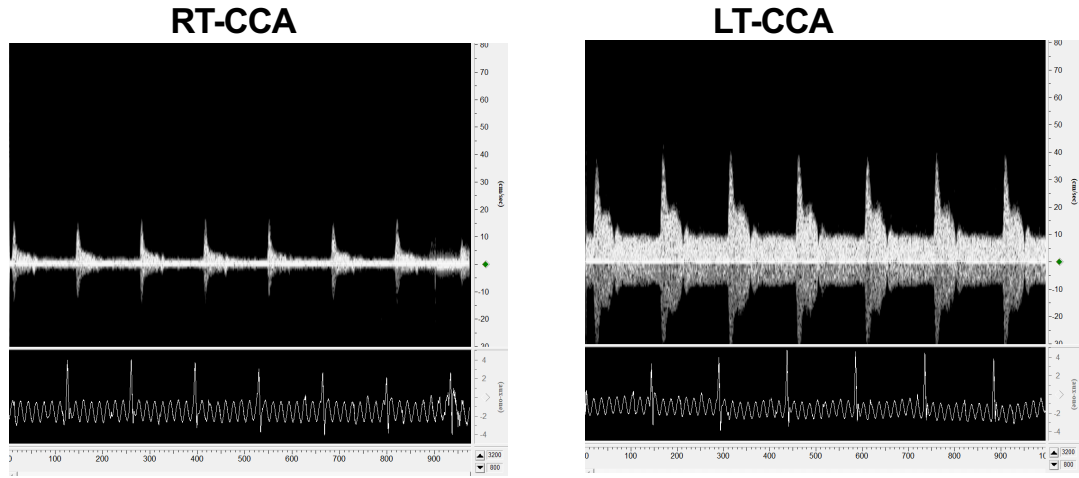
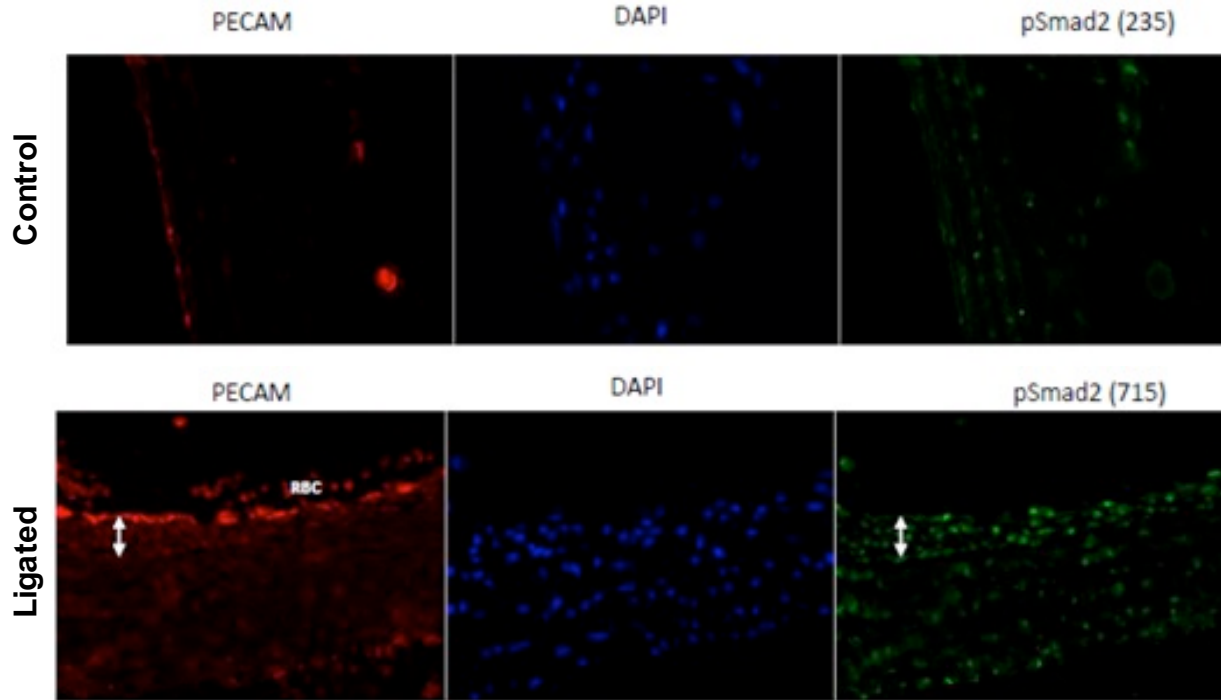


Figure S5. Carotid ligation in rats



RBC: red blood cells
(Average fluorescence of the endothelial cells)

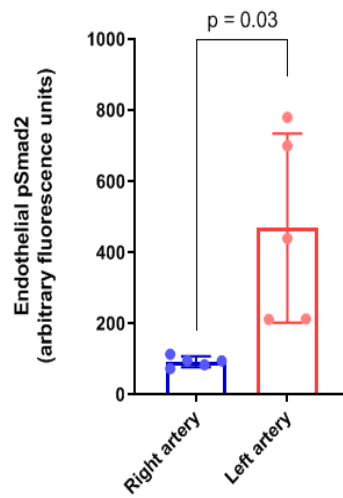
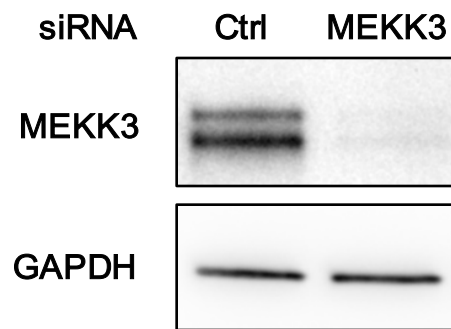


Figure S6. Knockdown confirmation

A



B

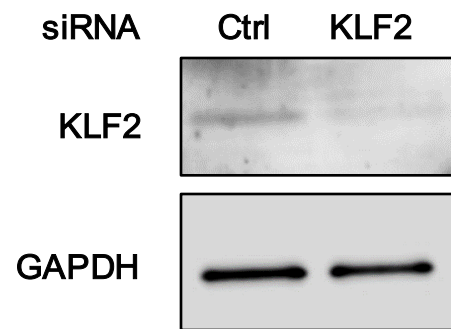


Figure S7. MEKK3 siRNA in MAECs

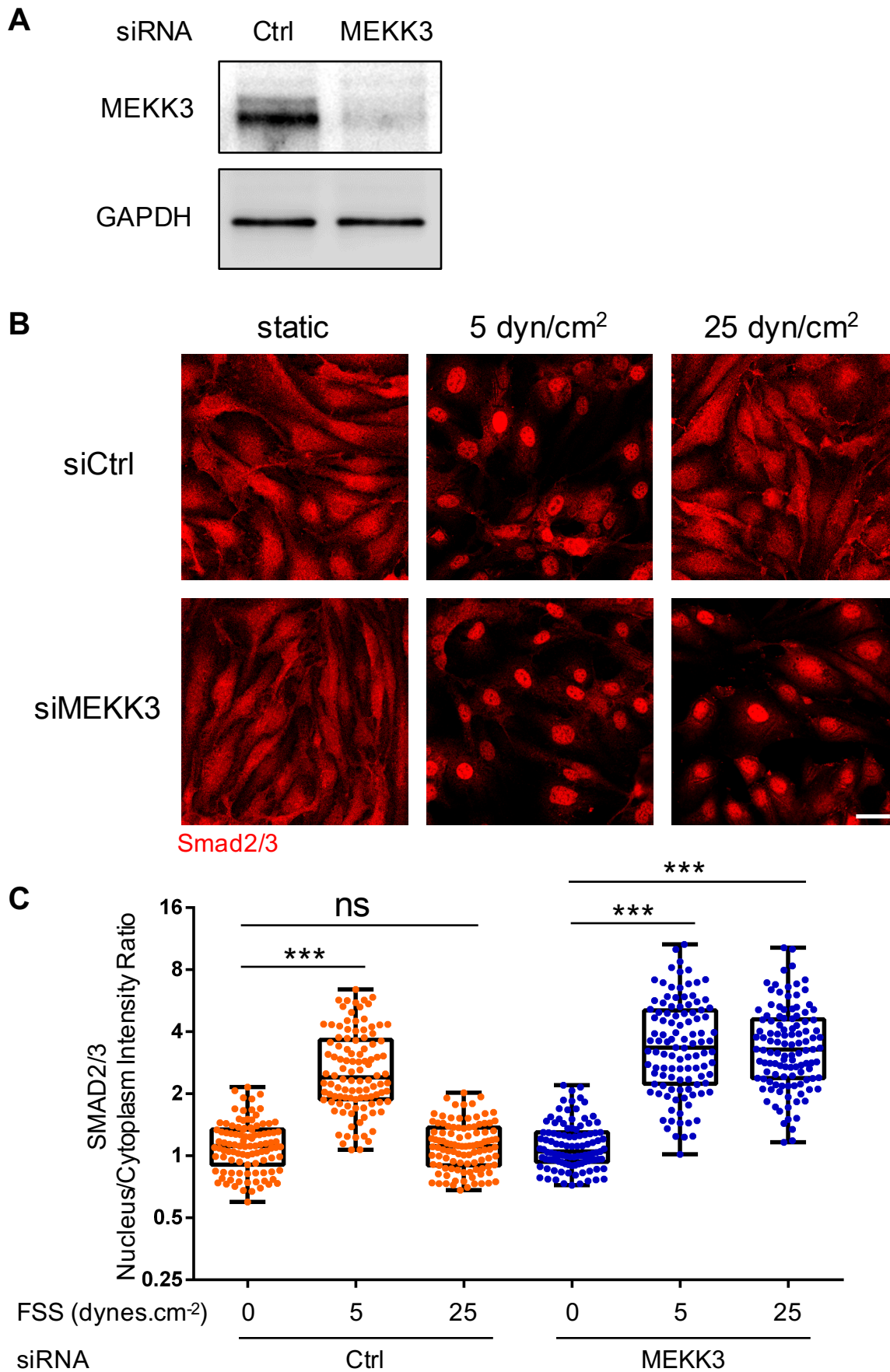


Figure S8. eNOS knockdown

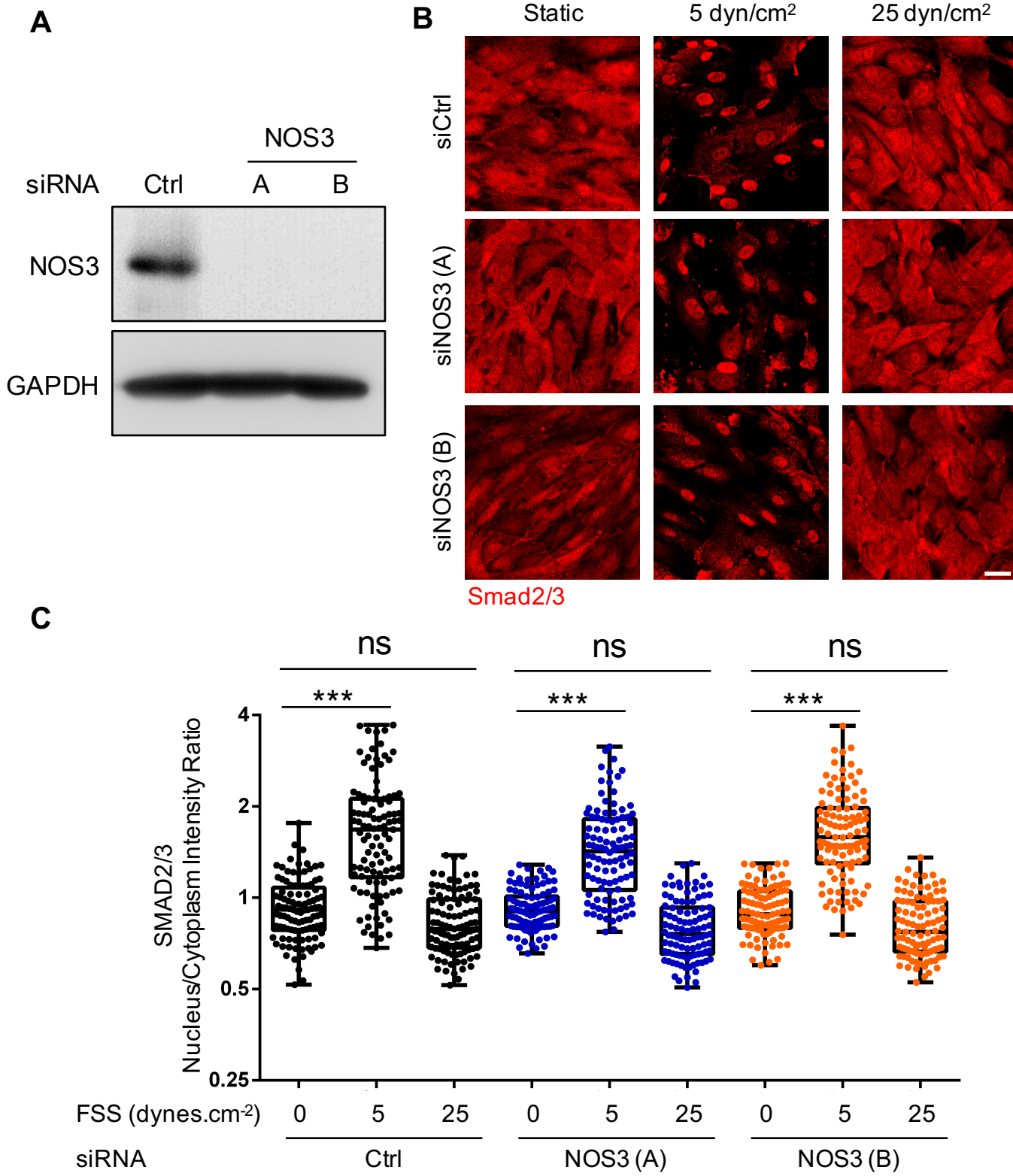


Figure S10. CDK2 activation time course

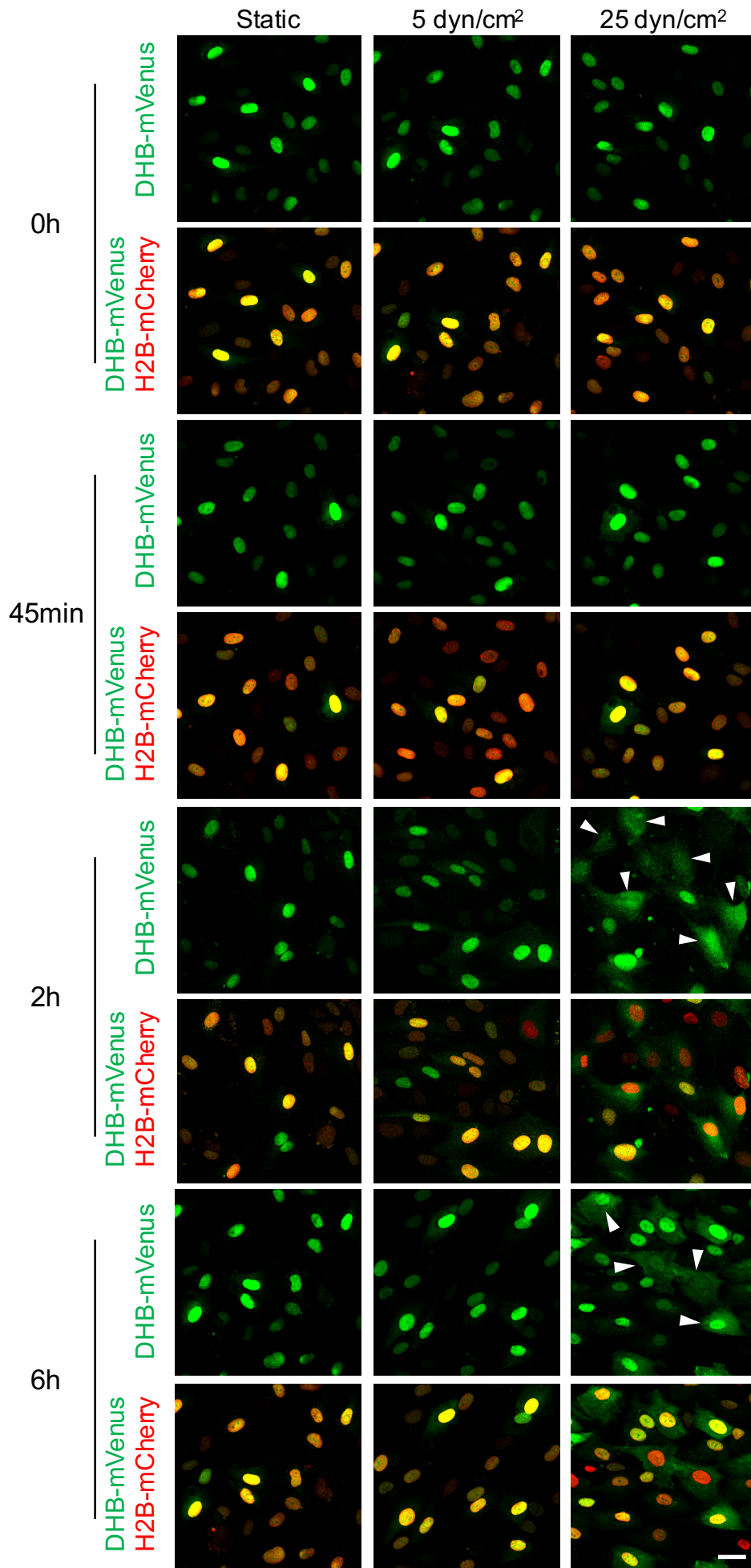
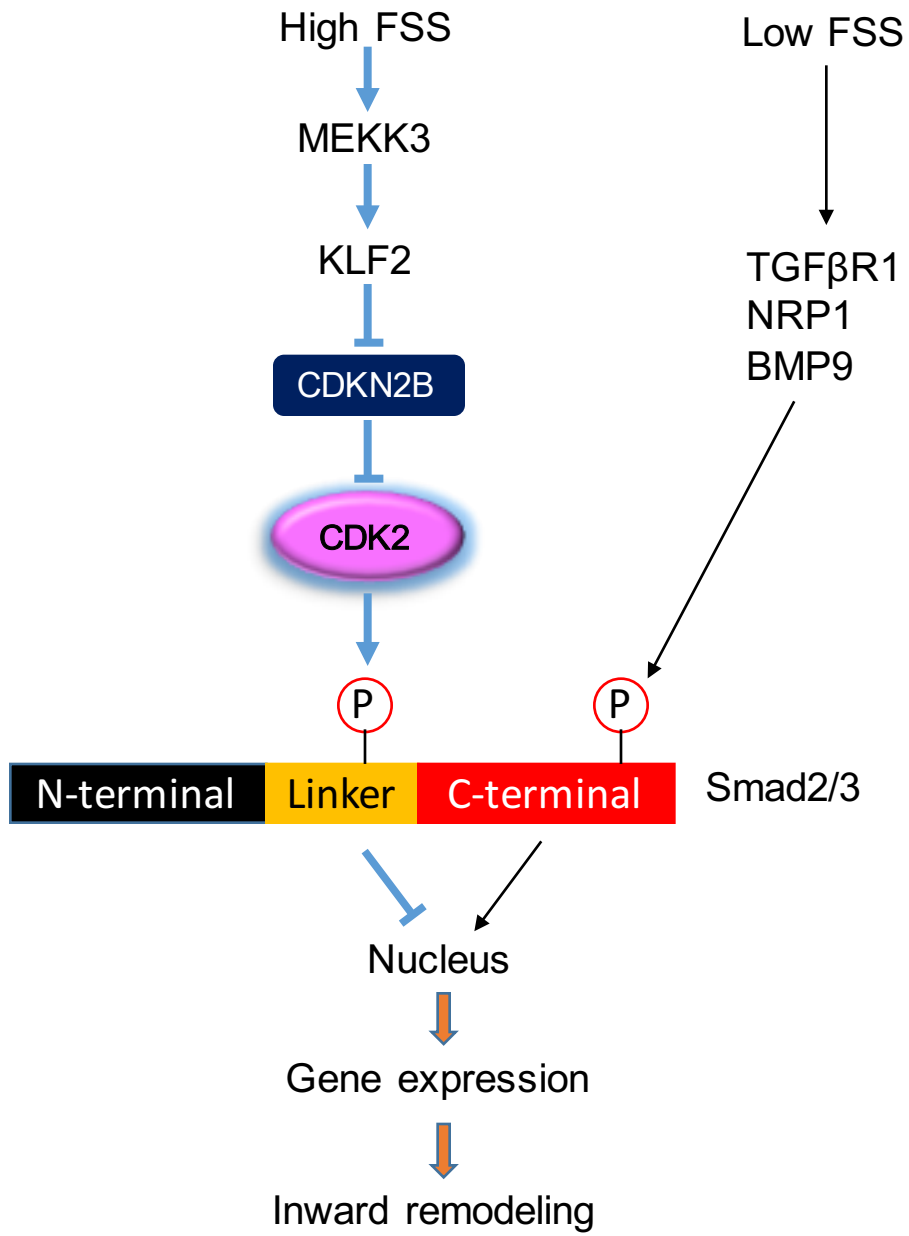


Figure S11. Pathway diagram



Supplemental Table 1. KLF2 dependent genes from RNAseq database.

Functional category	Gene_name	log2(FoldChange)	pvalue	padj (FDR)
	KLF2	-3.170722104	1.91E-27	1.48E-25
SMC contractility	JAG1	1.202082283	2.11E-36	2.57E-34
	JAG2	0.950801461	1.08E-13	2.97E-12
	EDN1	0.738471705	1.40E-21	7.59E-20
	NOS3	-1.291343264	5.93E-17	2.15E-15
SMC growth and migration	SLIT3	1.194891761	1.59E-10	3.02E-09
	SLIT2	0.608032041	4.87E-08	6.22E-07
	PDGFD	0.945071877	1.80E-17	6.82E-16
	PDGFRB	-2.105707332	7.91E-17	2.84E-15
	PDGFC	1.07650055	8.92E-17	3.18E-15
	PDGFB	0.746200172	6.09E-07	6.31E-06
	PDGFRA	1.01954145	7.79E-07	7.87E-06
Matrix remodeling	MMP1	2.44601148	4.88E-145	1.38E-141
	MMP10	2.130040615	5.84E-43	9.49E-41
	MMP28	-1.658791349	7.36E-27	5.45E-25
	MMP7	1.514666779	7.64E-17	2.75E-15
	MMP16	1.399351238	2.11E-11	4.59E-10
	MMP19	0.779468113	0.01241206	0.035978515
	TIMP3	1.217884096	1.91E-29	1.65E-27
	TIMP1	-0.491984505	0.0097276	0.029489566
Inflammatory genes	CCL2	2.005808955	1.46E-56	3.86E-54
	CCL14	-1.797455582	1.42E-24	9.38E-23
	CCL8	2.408505606	1.29E-15	4.16E-14
	CCL7	1.645065656	5.27E-11	1.08E-09
	CXCL1	3.569184582	1.10E-121	1.98E-118
	CXCL8	3.511492166	8.18E-116	1.25E-112
	CXCL5	3.88149904	2.01E-103	2.22E-100
	CXCL10	3.069317086	8.01E-76	4.29E-73
	CXCL3	2.119886834	1.69E-43	2.82E-41
	CXCL2	1.524274149	7.93E-40	1.14E-37
	CXCL6	3.191628473	1.14E-38	1.54E-36
	CXCL11	2.201781331	1.92E-25	1.34E-23
	IL1A	4.061189228	6.83E-100	5.89E-97
	IL1RL1	1.611791195	1.21E-96	8.59E-94
	IL7R	1.842205489	2.90E-45	5.09E-43
	IL16	1.761888431	4.71E-23	2.84E-21
IL6	1.544880616	1.30E-22	7.61E-21	